

# Effect of Ru substitution on atomic displacements in the layered $\text{SmFe}_{1-x}\text{Ru}_x\text{AsO}_{0.85}\text{F}_{0.15}$ superconductor

A. Iadecola,<sup>1</sup> B. Joseph,<sup>1</sup> L. Simonelli,<sup>2</sup> L. Maugeri,<sup>1</sup> M. Fratini,<sup>1</sup>

A. Martinelli,<sup>3</sup> A. Palenzona,<sup>3</sup> M. Putti,<sup>3</sup> and N. L. Saini<sup>1</sup>

<sup>1</sup>*Dipartimento di Fisica, Università di Roma “La Sapienza” - P. le Aldo Moro 2, 00185 Roma, Italy*

<sup>2</sup>*European Synchrotron Radiation Facility, BP220, F-38043 Grenoble Cedex, France*

<sup>3</sup>*CNR-SPIN and Università di Genova, via Dodecaneso 33, 16146 Genova, Italy*

The effect of Ru substitution on the local structure of layered  $\text{SmFe}_{1-x}\text{Ru}_x\text{AsO}_{0.85}\text{F}_{0.15}$  superconductor has been studied by As  $K$ - and Sm  $L_3$  - edges x-ray-absorption spectroscopy. The extended x-ray-absorption fine-structure measurements reveal distinct Fe-As and Ru-As bondlengths in the Ru substituted samples with the latter being  $\sim 0.03$  Å longer. Local disorder induced by the Ru substitution is mainly confined to the FeAs layer while the SmO spacer layer sustains a relative order, consistent with the x-ray-absorption near-edge structure spectra. The results suggest that, in addition to the order/disorder in the active iron-arsenide layer, its coupling to the rare-earth–oxygen spacer layer needs to be considered for describing the electronic properties of these layered superconductors.

Journal reference : *Physical Review B* **85** (2012) 214530

DOI: [10.1103/PhysRevB.85.214530](https://doi.org/10.1103/PhysRevB.85.214530)

PACS numbers: 74.70.Xa; 74.62.Dh; 61.05.cj; 78.70.Dm

## I. INTRODUCTION

Since the discovery of high- $T_c$  superconductivity in doped LaFeAsO, the iron-based superconductors continue to attract substantial interest of the condensed-matter community, producing a large amount of experimental and theoretical works [1–5]. Among these, the RFeAsO ( $R$  stands for rare-earth), the so-called 1111-type superconductors (with highest  $T_c$  of 55 K for the SmFeAsO $_{1-x}$ F $_x$ ), are highly studied materials. However, interplay of different electronic degrees of freedom makes it difficult to distinctly identify the role of different physical parameters governing the fundamental electronic structure of these superconductors. One of the key features is the layered structure with active FeAs layers separated by RO spacer layers. The fundamental electronic structure, characterized by Fe 3d interacting with the As 4p states [5], is generally manipulated by controlling the RO spacers, e.g. by substitution at the  $R$  site and/or by substitution at the O site [1–4]. In this regard, the interlayer interaction between the active FeAs layers and the spacer layers is of particular interest, with atomic disorder and local strain being the key issues. Earlier we have addressed these issues where properties of the 1111-system were manipulated by substitution at the  $R$  site, providing important information on the interaction between the two layers [6–9].

Recently, several efforts are made to manipulate the effect of disorder in the active FeAs layers by substitution. In particular, isovalent substitution at the Fe site [10–13] has been used to study the effect of disorder on the superconductivity. Apart from the effect on the superconductivity, these studies were also motivated by the possibility to answer the question of the symmetry of order parameter in the iron-based superconductors [14, 15], either in the spin-fluctuation approach [16–18] with anion height as a key parameter [18], or the orbital fluctuations mediated superconductivity with iron-phonons [19]. In this respect it is important to quantify the disorder induced by the isovalent substitution and to study its implication on the inter-layer correlations and electronic properties. Aiming to address these issues we have studied the local structure of SmFe $_{1-x}$ Ru $_x$ AsO $_{0.85}$ F $_{0.15}$  superconductors as a function of Ru substitution. At the optimum F doping, it has been found that the Ru substitution in the SmFe $_{1-x}$ Ru $_x$ AsO $_{0.85}$ F $_{0.15}$  strongly affects the  $T_c$  with a concomitant enhancement of the disorder as seen by transport measurements [10]. Interestingly, the short-range static magnetic order recovers with the Ru substitution, revealed by muon spin resonance ( $\mu$ SR) measurements [11]. Here, to investigate the nature of the local disorder, we have exploited atomic site selective x-ray-absorption spectra measured at the As  $K$ - and Sm  $L_3$ - edges providing direct information on the FeAs layers and the SmO spacer layers. We find that the local disorder induced by Ru substitution is mainly confined to the FeAs layers, revealed by the As  $K$ -edge extended x-ray-absorption fine-structure (EXAFS) measurements. On the other hand, x-ray-absorption near-edge structure (XANES) spectra at the As  $K$ - edge combined with Sm  $L_3$ -edge data indicate reduced disorder in the SmO spacer layer with increasing Ru substitution. These results underline the importance of spacer layers and the interlayer coupling in these layered superconductors.

## II. EXPERIMENTAL DETAILS

Polycrystalline samples of SmFe $_{1-x}$ Ru $_x$ AsO $_{0.85}$ F $_{0.15}$  ( $x = 0.0, 0.25$ , and  $0.5$ ) were used for the present study. Details on the sample preparation and characterization are given elsewhere [10]. The superconducting transition temperatures ( $T_c$ ) are 51, 14, and 8 K respectively for the samples with  $x = 0.0, 0.25$ , and  $0.5$ . The As  $K$ -edge ( $E = 11868$  eV) and Sm  $L_3$ -edge ( $E = 6717$  eV) x-ray-absorption measurements were performed in transmission mode at the beamline

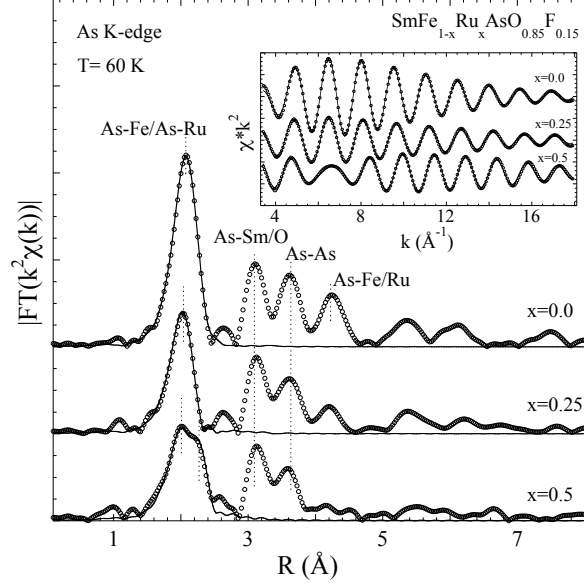


FIG. 1: Fourier transform (FT) magnitudes of the As  $K$ -edge EXAFS (weighted by  $k^2$ ) measured on  $\text{SmFe}_{1-x}\text{Ru}_x\text{AsO}_{0.85}\text{F}_{0.15}$  samples at 60 K (symbols) with the model fits (solid line) considering the nearest-neighbours (Fe/Ru shell). The FTs are performed in the  $k$ -range of  $3\text{--}18\text{\AA}^{-1}$  using a Gaussian window. The inset shows experimental filtered EXAFS oscillations (symbols) with the model fits (solid lines).

BM23 of the European Synchrotron Facility (ESRF), Grenoble. A minimum of five scans were acquired on each samples to ensure high signal to noise ratio and the spectral reproducibility. The EXAFS oscillations were extracted from the absorption spectra using standard procedure [20]. While the As  $K$ -edge EXAFS could be obtained up to high  $k$ -value, the  $k$ -range of the Sm  $L_3$ -edge EXAFS was limited by the Fe  $K$ -edge absorption jump at 7112 eV. The XANES spectra were normalized to the atomic absorption estimated by a linear fit to the data in the EXAFS region after a pre-edge background subtraction.

### III. RESULTS AND DISCUSSIONS

Figure 1 shows Fourier transform (FT) magnitudes of the As  $K$ -edge ( $k$  range 3 - 18  $\text{\AA}^{-1}$ ) EXAFS oscillations, measured on  $\text{SmFe}_{1-x}\text{Ru}_x\text{AsO}_{0.85}\text{F}_{0.15}$  at 60 K, providing partial atomic distribution around the As atoms. There are four Fe/Ru near neighbours of arsenic at a distance  $\sim 2.4$   $\text{\AA}$  and their contribution appears as the main peak in the FT at  $\sim 2$   $\text{\AA}$ . The next nearest neighbours of arsenic are Sm ( $\sim 3.3$   $\text{\AA}$ ) and O/F ( $\sim 3.5$   $\text{\AA}$ ) atoms, followed by the As atoms at  $\sim 3.9$   $\text{\AA}$ . Contributions of these distant shells appear mixed with the multiple scattering contribution due to Fe/Ru ( $\sim 4.6$   $\text{\AA}$ ), appearing as FT peaks in the range  $\sim 3\text{--}5$   $\text{\AA}$ . The amplitude of the main FT peak is strongly damped with the Ru substitution. Compared to this, the FT peak due to As-Sm/O shows negligible change while the As-As scattering appears to suffer a small decrease. In the sample with  $x = 0.25$ , the As-Fe/Ru peak is decreased by almost half and appears as a clear doublet structure in the sample with  $x = 0.5$ . Also the multiple scattering peak due to As-Fe/Ru sustains large change, almost disappearing for the sample with  $x = 0.5$ . These observations suggest that the atomic disorder introduced by the Ru is confined mainly to the FeAs layer, with minor influence on the SmO

spacer layer.

To quantify the disorder, we have analyzed the first shell EXAFS containing contribution only due to the As-Fe/Ru bonds, well separated from other contributions. In the single-scattering approximation, the EXAFS amplitude is described by the following general equation [20]:

$$\chi(k) = \sum_i \frac{N_i S_0^2}{k R_i^2} f_i(k, R_i) e^{-\frac{2R_i}{\lambda}} e^{-2k^2 \sigma_i^2} \sin[2k R_i + \delta_i(k)]$$

where  $N_i$  is the number of neighbouring atoms at a distance  $R_i$  from the photoabsorber.  $S_0^2$  is the passive electrons reduction factor,  $f_i(k, R_i)$  is the backscattering amplitude,  $\lambda$  is the photoelectron mean free path,  $\delta_i$  is the phase shift, and  $\sigma_i^2$  is the correlated Debye-Waller factor (DWF) measuring the mean-square relative displacements (MSRDs) of the photoabsorber-backscatterer pairs.

The filtered EXAFS oscillations are displayed as the inset of the Fig. 1, revealing clear damping with Ru substitution. In the model fits we have varied the As-Fe/Ru distances and the Debye-Waller factor ( $\sigma^2$ ), while all other parameters (photo-electron energy origin  $E_0$ , the number of near neighbors  $N_i$  and  $S_0^2$ ) were kept fixed in the least squares modelling with structural input from diffraction studies [10]. Phase shifts and amplitude factors were calculated using the `FEFF` code [21]. The number of independent data points for this analysis was 11 ( $N_{ind} \sim (2\Delta k \Delta R)/\pi$ , where  $\Delta k = 15 \text{ \AA}^{-1}$  and  $\Delta R = 1.2 \text{ \AA}$  are the ranges in  $k$  and  $R$  space over which the data are analyzed) for the two (four) parameters fit to the EXAFS of unsubstituted (substituted) sample.

TABLE I: Near neighbour distances and their  $\sigma^2$  measured by EXAFS for the  $\text{SmFe}_{1-x}\text{Ru}_x\text{AsO}_{0.85}\text{F}_{0.15}$  as a function of Ru substitution ( $T = 60 \text{ K}$ ). The average uncertainties, determined by correlation maps, are  $\pm 0.006$  and  $\pm 0.0004$  respectively for the distances and  $\sigma^2$  determined by the As  $K$ -edge. The uncertainties for the parameters obtained by the Sm  $L_3$  edge are almost twice those for the As  $K$  edge.

	$R_{Fe-As}(\text{\AA})$	$\sigma_{Fe-As}^2(\text{\AA}^2)$	$R_{Ru-As}(\text{\AA})$	$\sigma_{Ru-As}^2(\text{\AA}^2)$	$R_{Sm-O}(\text{\AA})$	$\sigma_{Sm-O}^2(\text{\AA}^2)$
$x = 0.0$	2.392	0.0030	-	-	2.288	0.0054
$x = 0.25$	2.387	0.0032	2.419	0.0030	2.285	0.0049
$x = 0.50$	2.390	0.0052	2.429	0.0025	2.291	0.0040

The bond distances and the  $\sigma^2$  (describing mean square relative displacements) obtained from the above analysis are given in Table I. The Fe-As distance is found to remain constant about  $\sim 2.39 \text{ \AA}$  for different  $x$ , however, this distance differs from the Ru-As distance, measured to be about  $\sim 2.42 \text{ \AA}$ . The difference between the two bonds ( $\sim 0.03 \text{ \AA}$ ) in this system is smaller than that measured ( $\sim 0.06 \text{ \AA}$ ) in the couples of isostructural compounds  $\text{RuAs} - \text{FeAs}$  and  $\text{RuAs}_2 - \text{FeAs}_2$  [22]. Thus, it appears that the  $\text{FeAs}_4$  ( $\text{RuAs}_4$ ) blocks are under chemical pressure in the 1111-structure by the  $RO$  layers. On the other hand, the Fe-As bond in these materials is known to be highly covalent [6]. In fact, this bond in the 1111 system hardly shows any change even with the changing rare-earth size [6, 23]. Again, the local Fe-As distance in  $\text{SmFe}_{1-x}\text{Ru}_x\text{AsO}_{0.85}\text{F}_{0.15}$  with Ru substitution remains constant, consistent with its highly covalent nature. Incidentally, the corresponding  $\sigma^2$  for the Fe-As bond lengths are similar for samples with  $x = 0.0$  and  $0.25$ , even if there is a clear increase in  $\sigma^2$  of this bond for the  $x = 0.50$  sample, with a small decrease of  $\sigma^2$  for the Ru-As bonds (Table I). It is known that, while the  $T_c$  of the  $\text{SmFe}_{1-x}\text{Ru}_x\text{AsO}_{0.85}\text{F}_{0.15}$  decreases from 51 to 14 K with  $x = 0$  to  $x = 0.25$ , the residual resistivity increases with a local maximum around  $x = 0.25$ , that has been assigned to impurity scattering in the system [10]. Incidentally, the residual resistivity decreases from  $x = 0.25$

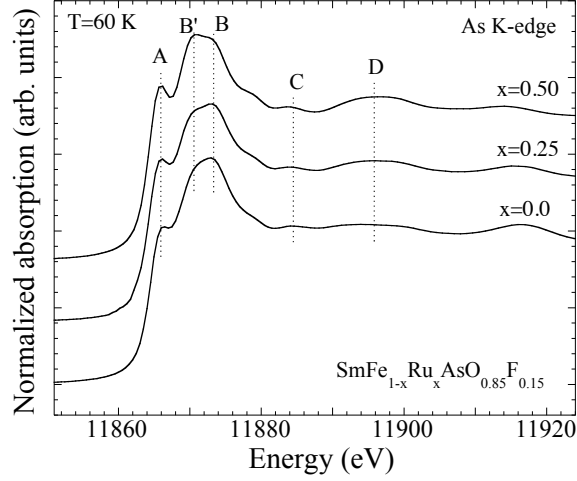


FIG. 2: Arsenic  $K$ -edge XANES of  $\text{SmFe}_{1-x}\text{Ru}_x\text{AsO}_{0.85}\text{F}_{0.15}$  measured at 60 K. Different near edge features are marked as A, B', B, C and D.

to 0.5, while the  $T_c$  shows a smaller change from 14 to 8 K [10]. Therefore, in the light of present findings, it is likely that the  $x = 0.5$  sample gets phase separated unlike the samples with  $x \leq 0.25$  in which the Ru appear as impurity centers.

Being a probe of higher order atomic correlations, the XANES measurements provide important information on the local geometry. Figure 2 shows the As  $K$ -edge XANES spectra of the  $\text{SmFe}_{1-x}\text{Ru}_x\text{AsO}_{0.85}\text{F}_{0.15}$  samples. Different near edge features are marked as A, B', B, C and D. The ground state electronic configuration of As atom is  $[\text{Ar}]3d^{10}4s^24p^3$  and the As  $K$ -edge spectra probes the transition of core  $1s$  electrons to the empty  $p$  states. Multiple scattering (MS) calculations of As  $K$ -edge XANES features for  $R\text{FeAsO}$  have shown that the absorption feature A has predominant As  $4p$  character with admixed Fe/Ru  $d$  states. Similarly, the feature B is due to As  $4p$  admixed with Fe/Ru  $p$  states. Also, the distant features C and D appear to have predominantly As  $4p$  character [8]. With increased Ru doping the intensity of the feature A increases, indicating increased unoccupied states of  $p$ -symmetry, merely due to the extended Ru  $4d$  states compared to the Fe  $3d$  states, and hence larger mixing with the As  $4p$  states. MS calculations have further revealed that the feature B' is correlated with the local geometry of the  $RO$  spacers. Indeed this feature is relatively intense in the As  $K$ -edge XANES spectrum for larger  $R$  (e.g.,  $\text{LaFeAsO}$ ) with respect to the smaller  $R$  (e.g.,  $\text{SmFeAsO}$ ) system. This is due to higher local disorder of  $RO$  layer in the system with smaller  $R$  size (i.e., SmO) with respect to the system with larger  $R$  (i.e., LaO) [7, 8]. The feature B' in the spectra of  $\text{SmFe}_{1-x}\text{Ru}_x\text{AsO}_{0.85}\text{F}_{0.15}$  gets intense with increasing Ru substitution that is an indication of reduced disorder in the SmO spacer layer. In this respect, it appears that the effect of the Ru substitution in the FeAs layer is similar to the one with increasing rare-earth size [7, 8] (i.e., reduced disorder in the  $RO$  spacer). Therefore, the oxygen order/disorder in the  $RO$  spacer layer should have significant role in the properties of  $\text{SmFe}_{1-x}\text{Ru}_x\text{AsO}_{0.85}\text{F}_{0.15}$  as well.

To address the question of order/disorder in the spacer layer, we have directly measured the atomic correlations by Sm  $L_3$ -edge absorption spectroscopy. Figure 3 shows FT magnitudes of the Sm  $L_3$ -edge ( $k$  range 3 - 9.0  $\text{\AA}^{-1}$ ) EXAFS oscillations at 60 K, providing the atomic distribution around Sm. For the Sm site, there are four O near neighbours

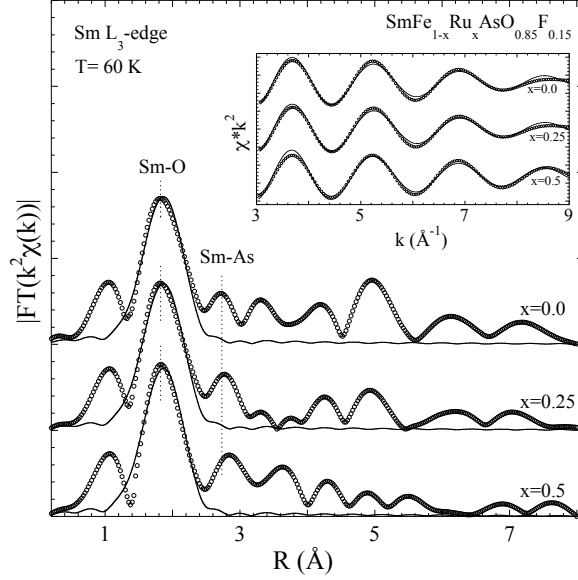


FIG. 3: Fourier transform (FT) magnitudes of the Sm  $L_3$ -edge EXAFS (weighted by  $k^2$ ) measured on  $\text{SmFe}_{1-x}\text{Ru}_x\text{AsO}_{0.85}\text{F}_{0.15}$  ( $x=0.0, 0.25, 0.5$ ) samples at 60 K (symbols) with the model fits (solid line). The FTs are performed in the  $k$ -range of 3.0-9.0  $\text{\AA}^{-1}$  using a Gaussian window. The inset shows experimental filtered EXAFS oscillations with the model fits (solid lines).

at a distance  $\sim 2.3$  Å (main peak at  $\sim 1.8$  Å). The next neighbours of Sm are four As atoms at a distance  $\sim 3.3$  Å, and Fe atoms at a distance  $\sim 3.6$  Å. An apparent shift of the Sm-As FT peak position may be due to increasing Sm-As distance, consistent with the As  $K$ -edge EXAFS, however limited  $k$ -range of the data does not permit us to make any further quantification. Here, we focus only on the Sm-O bonds, the contribution of which is well separated from the contributions of the distant shells and hence can be analysed using a single shell model. The filtered Sm-O EXAFS oscillations are also included in Fig. 3 (inset). Following a similar approach as above, we have kept fixed all the parameters except the Sm-O distance and the  $\sigma^2$ . The number of independent data points for this analysis was about 4 for the two parameters fit. Although the  $k$ -range is limited, a single shell analysis with two parameters can still provide useful information on the near neighbor displacements with a good confidence level. The Sm-O distance and its  $\sigma^2$ , determined by the single shell modeling, are included in the Table I. The results suggest that the Sm-O distance remains constant within the experimental uncertainties, however, the  $\sigma^2$  tend to decrease with the Ru substitution. This implies that the local disorder in the SmO layer is getting reduced, consistent with the conclusions drawn on the basis of As  $K$ -edge XANES (Fig. 2).

To have further information, we have analyzed the Sm  $L_3$ -edge XANES spectra. Figure 4 shows normalized Sm  $L_3$ -edge XANES spectra measured on  $\text{SmFe}_{1-x}\text{Ru}_x\text{AsO}_{0.85}\text{F}_{0.15}$  as a function of Ru substitution. The spectra show an intense peak, the characteristic white line (W) of  $\text{Sm}^{3+}$  due to  $2p_{3/2} \rightarrow 5\epsilon d$  transition. The other near edge features are denoted by  $A_1$ ,  $B_1$  and  $B_2$ , appearing around 15 eV, 35 eV, 50 eV above the white line. Compared to the As  $K$ -edge XANES the changes in the Sm  $L_3$ -edge spectra are much smaller, confirming once again that the main effect of the Ru substitution is confined to the FeAs layer. The features  $B_1$  and  $B_2$  are continuum resonance peaks [7] due to scatterings with As at  $\sim 3.3$  Å and O at  $\sim 2.3$  Å. MS calculations of RE  $L_3$ -edge in the 1111 system have shown that the feature  $A_1$  is sensitive to the order/disorder in the SmO plane [8]. Although small, there are few apparent changes

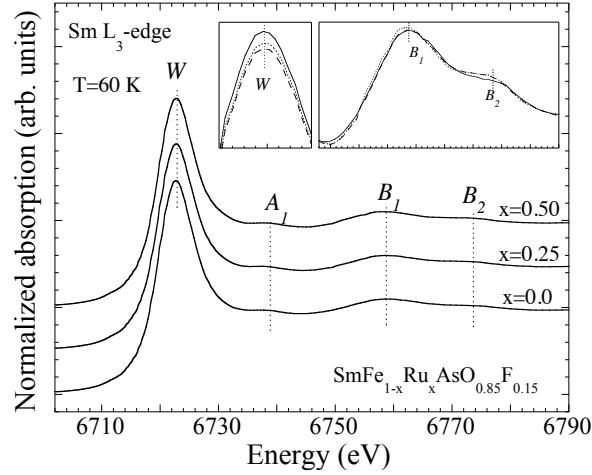


FIG. 4: Sm  $L_3$ -edge XANES spectra of  $\text{SmFe}_{1-x}\text{Ru}_x\text{AsO}_{0.85}\text{F}_{0.15}$  ( $x = 0.0, 0.25$ , and  $0.5$ ). The whiteline is indicated by  $W$  while other near edge features are marked as  $A$ ,  $B_1$  and  $B_2$ . The insets show zoom over the whiteline (left) and the features  $A$ ,  $B_1$  and  $B_2$  (right). The solid, dashed and dotted lines in the insets correspond to the spectra of  $x = 0.0, 0.25$ , and  $0.5$  respectively.

in the XANES features. While the  $B_1$  shifts towards lower energy, the  $B_2$  appears to gain some intensity with Ru substitution (inset in Fig. 4). The shift of  $B_1$  is due to increased Sm-As distance, consistent with the EXAFS. On the other hand, the increased intensity of the  $B_2$  indicates reduced disorder in the SmO sublattice with Ru substitution, again consistent with the EXAFS data.

In summary, we have studied the local structure of the superconducting  $\text{SmFe}_{1-x}\text{Ru}_x\text{AsO}_{0.85}\text{F}_{0.15}$  system with variable Ru by x-ray absorption measurements. The EXAFS and XANES spectra obtained at the As  $K$ - and Sm  $L_3$ -edges have permitted to obtain information on the local structure of the active FeAs layers and the SmO spacer layers. The EXAFS data reveal distinct Fe-As and Ru-As bondlengths and the local disorder being confined in the FeAs layer, while the SmO spacer layer sustaining a local order. Therefore, the effect of Ru substitution in the FeAs layer appears similar to what has been found in the rare-earth substituted  $R\text{FeAsO}$  with different rare-earth size [6–8]. It was found that the coupling between the two layers gets weaker for bigger size of rare-earth while the FeAs layers getting thinner, similar to the increasing Ru substitution at the Fe site seen in this work.

The decoupling of the two layers means that the two sublattices are independent and the active FeAs layer loses screening from the spacer  $RO$  layer due to smaller interlayer coupling in the Ru substituted system. On the other hand, the FeAs layers get thinner, consistent with diffraction [10], and electronically the system acts as a 11-type superconductor (i.e., a binary FeSe), albeit with smaller pnictogen height from the Fe-plane, i.e., more three-dimensional character of the band structure (larger  $k_z$ -dispersion as seen by angle resolved photoemission [24]) near the Fermi level that is mainly derived by the Fe  $3d$  admixed As  $4p$  orbitals. Smaller interlayer coupling also means that the substituted Ru atoms in the FeAs layers acting as localized disorder due to poorer screening and/or there is a phase separation similar to the one appears in the ternary  $\text{FeSe}_{1-x}\text{Te}_x$  systems on Te substitution [25]. Here, it seems that the impurity scattering due to the atomic disorder being partly responsible for the  $T_c$  suppression, also evident from the residual resistivity behaviour with the Ru concentration [10]. Since residual resistivity decreases as



well the interlayer coupling with further Ru concentration ( $x \geq 0.25$ ), it is likely that the static disorder prevails while the system gets phase separated with reentrant local magnetic order [11]. In the present case, the  $T_c$  decreases from 51 to 14 K with smaller amounts of Ru substitution ( $x = 0.0$  to 0.25), while the  $T_c$  change is smaller, from 14 to 8 K, with larger amounts of Ru substitution (for  $x = 0.25$  to 0.5). Therefore different mechanisms appears to be active for the  $T_c$  suppression with different concentration ranges for the isoelectronic substitution. In conclusion, the present results demonstrate importance of interlayer atomic correlations for describing the electronic properties of the layered 1111-type superconductors. Having direct implication on spin/orbital fluctuation theories [14–19], these topological aspects need proper consideration for a realistic description of the superconductivity in these materials.

### Acknowledgments

Experimental support by the beamline staff at the ESRF is kindly acknowledged. The work at Genova is partially supported by FP7 SUPER-IRON Project (No.283204).

- 
- [1] D. C. Johnston, [Advances in Physics](#) **59**, 803 (2010).
  - [2] G. R. Stewart, [Reviews of Modern Physics](#) **83**, 1589 (2011).
  - [3] P. C. Canfield and S. L. Bud'ko, [Annual Review of Condensed Matter Physics](#) **1**, 27 (2010).
  - [4] H. H. Wen and S. Li, [Annual Review of Condensed Matter Physics](#) **2**, 121 (2011).
  - [5] O.K. Andersen and L. Boeri, [Annalen der Physik](#) **523**, 8 (2011).
  - [6] A. Iadecola, S. Agrestini, M. Filippi, L. Simonelli, M. Fratini, B. Joseph, D. Mahajan and N. L. Saini, [Europhysics Letters](#) **87**, 26005 (2009).
  - [7] B. Joseph, A. Iadecola, M. Fratini, A. Bianconi, A. Marcelli and N.L. Saini, [Journal of Physics: Condensed Matter](#) **21**, 432201 (2009); W. Xu, A. Marcelli, B. Joseph, A. Iadecola, W. S. Chu, D. Di Gioacchino, A. Bianconi, Z. Y. Wu, and N. L. Saini, [Journal of Physics: Condensed Matter](#) **22**, 125701 (2010).
  - [8] W. Xu, B. Joseph, A. Iadecola, A. Marcelli, W.S. Chu, D. Di Gioacchino, A. Bianconi, Z. Y. Wu and N. L. Saini, [Europhysics Letters](#) **90**, 57001 (2010).
  - [9] A. Ricci, B. Joseph, N. Poccia, W. Xu, D. Chen, W. S. Chu, Z. Y. Wu, A. Marcelli, N. L. Saini, and A. Bianconi, [Superconductor Science and Technology](#) **23**, 052003 (2010).
  - [10] M. Tropeano, M. R. Cimberle, C. Ferdeghini, G. Lamura, A. Martinelli, A. Palenzona, I. Pallecchi, A. Sala, I. Sheikin, F. Bernardini, M. Monni, S. Massidda, and M. Putti, [Physical Review B](#) **81**, 184504 (2010); I. Pallecchi, F. Bernardini, M. Tropeano, A. Palenzona, A. Martinelli, C. Ferdeghini, M. Vignolo, S. Massidda, M. Putti, [Physical Review B](#) **84**, 134524 (2011).
  - [11] S. Sanna, P. Carretta, P. Bonfa, G. Prando, G. Allodi, R. De Renzi, T. Shiroka, G. Lamura, A. Martinelli, and M. Putti, [Physical Review Letters](#) **107**, 227003 (2011).
  - [12] S. Kitagawa, Y. Nakai, T. Iye, K. Ishida, Y. F. Guo, Y. G. Shi, K. Yamaura, and E. Takayama-Muromachi, [Physical Review B](#) **83**, 180501 (2011).
  - [13] S. C. Lee, A. Kawabata, T. Moyoshi, Y. Kobayashi, and M. Sato, [Journal of the Physical Society of Japan](#) **78**, 043703 (2009); Y. Kobayashi, A. Kawabata, S. C. Lee, T. Moyoshi, and M. Sato, [Journal of the Physical Society of Japan](#) **78**, 073704 (2009); M. Sato, Y. Kobayashi, S. C. Lee, H. Takahashi, E. Satomi, and Y. Miura, [Journal of the Physical Society of Japan](#) **79**, 014710 (2010).



- [14] J. Hirschfeld, M. M. Korshunov and I. I. Mazin, [Report on Progress in Physics 74 124508 \(2011\)](#).
- [15] A. Chubukov, [Annual Review of Condensed Matter Physics 3,57 \(2012\)](#).
- [16] I. I. Mazin, D. J. Singh, M. D. Johannes, and M. H. Du, [Physical Review Letters 101, 057003 \(2008\)](#).
- [17] A.F. Kemper, T.A. Maier, S. Graser, H-P. Cheng, P.J. Hirschfeld and D.J. Scalapino, [New Journal of Physics 12, 073030 \(2010\)](#).
- [18] K. Kuroki, H. Usui, S. Onari, R. Arita, and H. Aoki, [Physical Review B 79, 224511 \(2009\)](#).
- [19] H. Kontani and S. Onari, [Physical Review Letters 104, 157001 \(2010\)](#).
- [20] X-ray Absorption: Principles, Applications, Techniques of EXAFS, SEXAFS, XANES, edited by R. Prins and D. C. Koningsberger (Wiley, New York, 1988).
- [21] J. Mustre de Leon, J. J. Rehr, S. I. Zabinsky, and R. C. Albers, [Physical Review B 44, 4146 \(1991\)](#); J. J. Rehr and R. C. Albers, [Reviews of Modern Physics 72, 621 \(2000\)](#).
- [22] R.D. Heyding, L.D. Calvert, [Canadian Journal of Chemistry 35, 449 \(1957\)](#); R.D. Heyding, L.D. Calvert, [Canadian Journal of Chemistry 39, 955 \(1961\)](#).
- [23] A. Martinelli, A. Palenzona, M. Tropeano, C. Ferdeghini, M. R. Cimberle, and C. Ritter, [Physical Review B 80, 214106 \(2009\)](#).
- [24] N. Xu, T. Qian, P. Richard, Y.-B. Shi, X.-P. Wang, P. Zhang, Y.-B. Huang, Y.-M. Xu, H. Miao, G. Xu, G.-F. Xuan, W.-H. Jiao, Z.-A. Xu, G.-H. Cao, H. Ding, [arXiv:1203.4699v1](#) (unpublished).
- [25] B. Joseph, A. Iadecola, A. Puri, L. Simonelli, Y. Mizuguchi, Y. Takano, and N. L. Saini, [Physical Review B 82, 020502 \(2010\)](#).